How to Cite:
Ahmed, R. T., Ahmed, A. F., & Aadim, K. A. (2022). Study of spectroscopic analysis performed of laser produced Sn and Sn:Cr plasma. *International Journal of Health Sciences*, *6*(S9), 1974–1982. https://doi.org/10.53730/ijhs.v6nS9.12839

Study of spectroscopic analysis performed of laser produced Sn and Sn:Cr plasma

Raghad T. Ahmed
Medical Instrumentation Techniques Engineering Bilad Alriafidain, University College, Diyala, Iraq and Department of physics, College of Science, University of Baghdad, Iraq.
Corresponding author email: raghda@bauc14.edu.iq

Ala F. Ahmed
Department of Astronomy & Space, College of Science, University of Baghdad, Iraq.
Email: ala.ahmed@sc.uobaghdad.edu.iq

Kadhim A. Aadim
Department of physics, College of Science, University of Baghdad, Iraq.

***Abstract*---**In this study, the LIBS technique was used to generate plasma from the Sn and Sn:Cr surfaces of these nanomaterials and to quantify the spectral emission of tin and chromium-containing tin. Nd-YAG laser has a wavelength of 1064 nm and a frequency of 6 Hz. After computing the plasma parameters, it was determined that the electron temperature is plasma Sn(1.286–1.819)ev and Sn: Cr (1.661-2.11505922)ev. The Sn(1.65-2.40) 108 cm -3 plasma electron density was also detected. Plasma Sn:Cr (2.85-3.39) 108cm-3 Additionally, calculations were made for plasma properties such plasma frequency, Debye length, and Debye number. At atmospheric pressure, the spectrum range of laser-induced plasma emission (200-1100 nm) was determined.

***Keywords*---**Laser-induced breakdown spectroscopy (LIBS), Optical Emission spectrum (OES), Sn plasma, Sn-Cr plasma.

1. Introduction

LIBS (laser-induced breakdown spectroscopy) It is a common tool to support accurate quantitative physical analysis in the field. The energy source is high-energy laser pulses. This means that any substance can be analyzed, regardless of its physical state - gaseous, solid or liquid. It

uses laser-mediated plasma emission signals to track specific types of atoms and molecules (Abbas & Saif, 2017). The target surface of the laser is quickly ionized to generate a plasma by an ablation process and a pulsed period laser (>1ns) laser interaction with the material. The laser light is absorbed by the electron target and, after interacting with the material's atoms, takes on the properties of an isothermal plasma if the incident plasma's time scale is less than the pulse duration (Apaydin & Celik, 2019; Shaikh et al, 2010). Latest analysis has shown that LIBS has been used to analyze biological samples such as tissues, diverse forms of bacteria, gall stones and aerosols (Haverkamp et al, 2003; Hanif & Salik, 2014). LIP has a significant impact on optical emission spectroscopy. The prevalent technique for electronically producing plasma from plasma aroused species is considered (Harilal et al, 2005). Optical emission spectroscopy (OES) dynamics is one of the simplest and least invasive techniques for examining early plasma dynamics since it depends on the LIP inherent light emission and doesn't call for external activation. This benefit makes setting up OES experiments simpler and makes automation and remote sensing easier. OES allows for the direct observation of the emission spectrum to gather fundamental cloud information (Wadaa, Ala & Aadim, 2020). The Boltzmann diagram can be used to compute the plasma electron temperature (Te). The following equation is then used to calculate the electron temperature (Te) (Ala et al, 2022).

$$Ln\left(\lambda_{ji} I_{ji} / g_j A_{ji}\right) = -\left(E_j / k_B T\right) + C \quad \text{..... (1)}$$

Where Iji denotes intensity, λji,and Aji denote wavelength and transition probability related to the change from I to j, respectively, and gi denotes statistical weight. The Boltzmann constant (KB), the constant (c), the excitation energy (Ej), and the temperature (Te) are all defined. The electron temperature is determined by taking the inverse of the slope of the Boltzmann plot[9]. The maximum width of height (FWMH) required to calculate the electron number density can be determined using the Stark expansion method [8].

$$n_e\ (cm^{-3}) = \left(\frac{\lambda_{FWHM}}{2\omega}\right) \times 10^{16} \quad \text{..... (2)}$$

in which ω is the electron effect parameter and the rather broadened full-width spectrum at most height (FWMH) (nm). Once the electron temperature (Te) (eV) and electron quantity density (ne) (cm-3) are calculated, the Debye length (λD) (cm) may be calculated the use of the subsequent formula (Maryam, Shehab & Aadim, 2021).

$$\lambda_D = \left(\frac{\varepsilon_0 k_B T_e}{n_e e^2}\right)^{1/2} \quad \text{..... (3)}$$

where ε_0 is the vacuum permittivity, KB is the Boltzmann constant and e is the price of an electron

As decided with the aid of using the subsequent equation, the Debye number (Madyan et al, 2020).

$$\mathbf{N_D = \frac{4\pi}{3}\lambda_D^3\, n_e} \quad \ldots\ldots\ldots\ldots \qquad (4)$$

The following equation can also be used to calculate the plasma frequency. (Maryam, Shehab & Aadim, 2021; Madyan et al, 2020).

$$f_p = \left(\frac{n_e e^2}{\varepsilon_0 m_e}\right)^{1/2} \quad \ldots\ldots\ldots\ldots \qquad (5)$$

The electron rest mass is represented by me.

2. Experimental Part

With a laser-to-target distance of 10 cm, Figure 1 depicts the experimental setup for laser-induced plasma spectroscopy (LIPS). The pulse duration was 9 ns, the repetition rate was 6 Hz, and the wavelength was 1064 nm, accurately measuring the gap between the precision and accuracy of the device. The lens's focal length in this piece is 10 cm. Light from a pulsed laser bombarding the sample is used for spectrometer analysis. "Light from the ablation plasma" is collected by the fibers. In order to prevent splatter, the fiber was positioned so that it was around 45 degrees off the axis of the laser beam before being fed through the spectrometer's entrance slit. for the spectral range, a spectrum analyzer (400 nm - 700 nm). In order to assess plasma parameters like electron temperature (T_e) and electron density (n_e) and determine plasma attributes, the results are examined and contrasted with data from the National Institute of Standards and Technology (NIST) (Kramida et al, n.d.).

In this work, tin samples weighing 2 g were prepared and tin and chromium were mixed in the specified ratio of Sn(1.4) to Cr(0.6). Both materials were of very high purity up to 99.99%. Tin and tin with chromium were pressed inside a stainless steel mold and pressed and it was at room temperature By a hydraulic press about 6 tons, tin and chromium tablets were obtained with a thickness of 2 mm. The emission spectra of tin-oriented tin plasma produced by the interaction of tin with curium-oriented tin at various laser peak energies from a tuned Q-Nd:YAG laser to the pulse were measured using the optical emission spectroscopy (OES) technique. derived from atmospheric sources. Record. Many distinctive spectral lines of a certain atom in the spectral region (200-1100 nm) make up the spectrum.

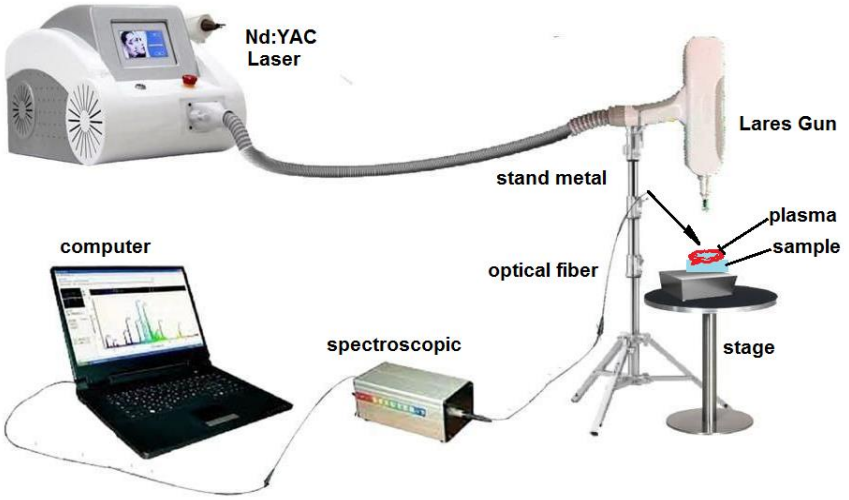

Figure 1. Diagrammatic representation of LIBS system.

3. Results and Discussion

The emission spectra of Sn plasma from various laser energies at atmospheric pressure is shown in Figure (2). Many characteristics can be show in this figure the emission spectra at wavelength between 240.9,288.9,283,303.2,332.2,365,397.7nm.The SnII ionic emission line between 452.4,498.6,590.644.1and 906.1nm. We note that the intensity increases as the laser energy increases. The typical emission line of SnI is considerably more potent than that of SnII. These consequences suggest that the generated plasma has a better awareness of atomic Sn than ionic Sn. This fact is understandable because, according to the plasma formation process, ionization occurs only a fraction of a millisecond before sputtering. The electrons that atoms expelled during ionization are thus further detained by ions during the recombination process. The ions consequently emit their energy as photon emissions as a result of recombination. Additionally, due to their different atomic number and high ionization energy (high ionization energy is needed), Sn atoms have a low ionization potential. These spectral traces are emitted whilst the tow factors combine, consisting of tin and chromium, and we have a look at an boom in emission because the laser strength reaches the goal surface. The look of atoms and ionic factors in every detail within side the goal emission place relies upon at the ionization power of the goal atom, as proven in Figure (3).

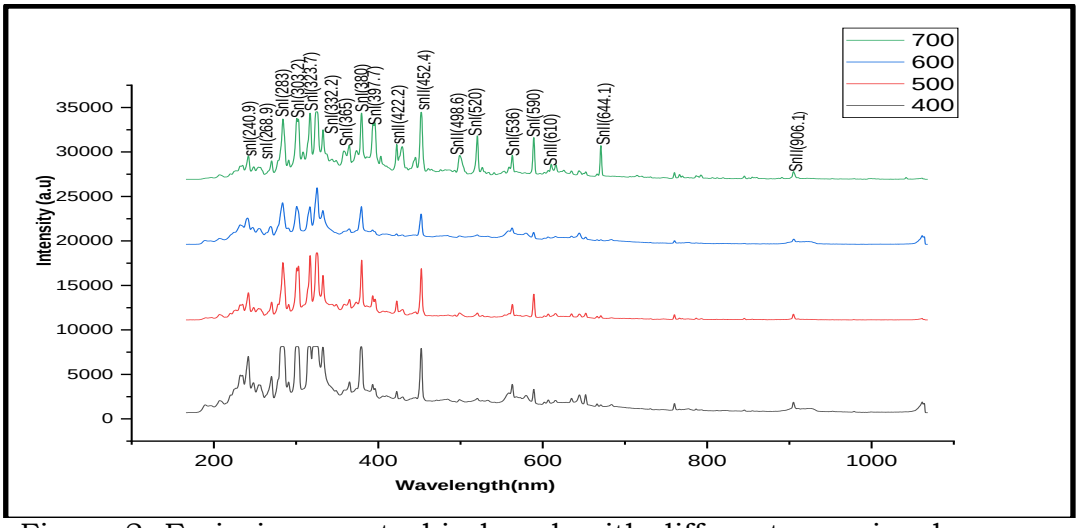

Figure 2. Emission spectral induced with different energies laser on the sn target.

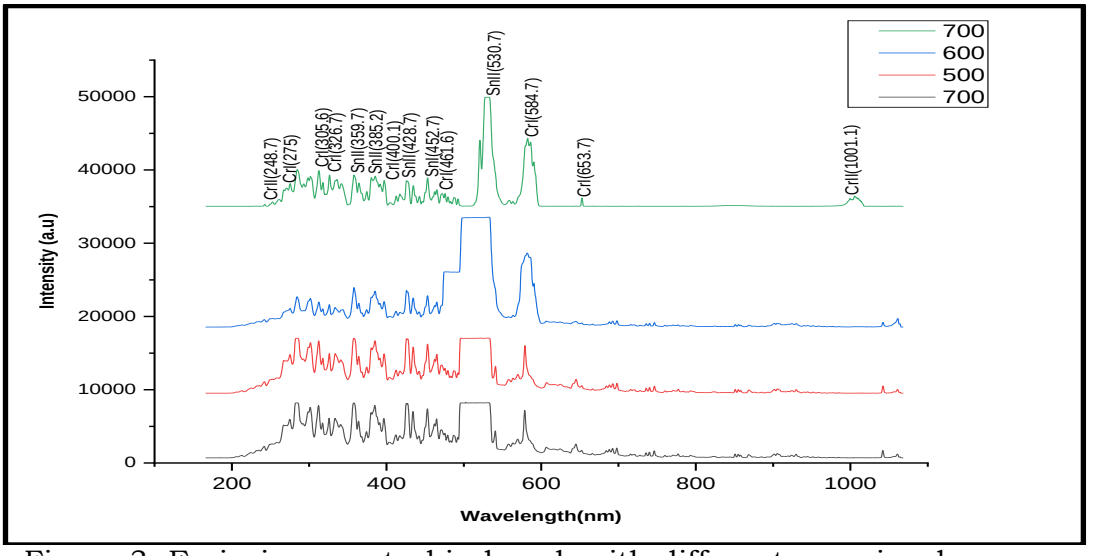

Figure 3. Emission spectral induced with different energies laser on the Sn:Cr target.

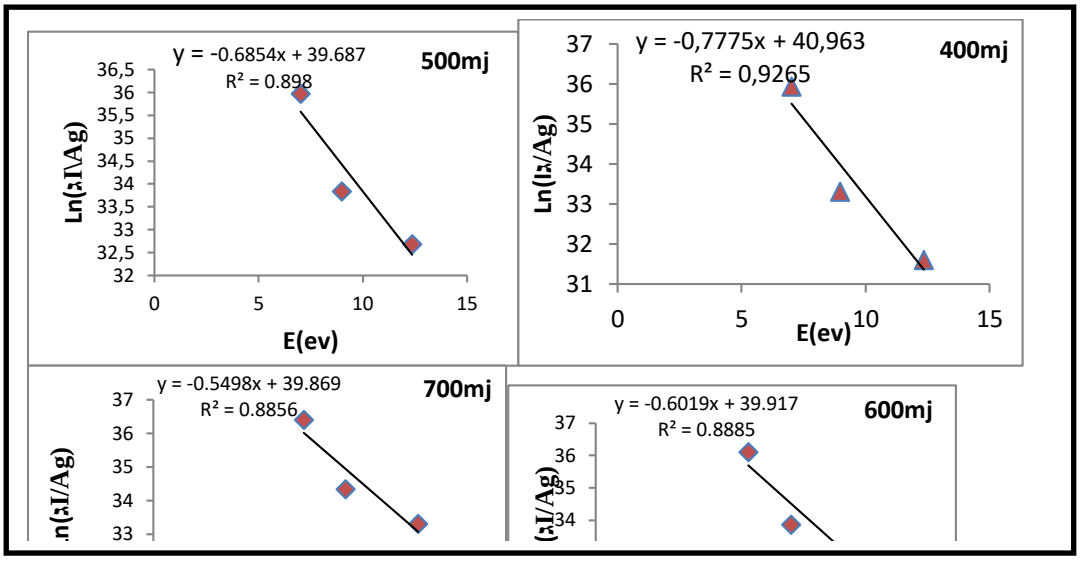

Figure 4. Boltzmann diagrams of Sn targets with different laser energies

The slope value is calculated by drawing a line between the highest energy level value according to (NIST) on the x-axis and the value $Ln(\lambda_{ji} I_{ji}/g_j A_{ji})$ on the y-axis, as shown in Figure 4). The behavior of electron plasma temperature and density with respect to laser energy induced on a Sn target is depicted in Figure 5 using a (1064 nm) laser. It is discovered that as laser power rises, electron temperature and density rise as well, with the electron density essentially remaining constant as the plasma opaque and protects the target from the laser beam. When the plasma itself lowers the maximum laser power provided along the beam path, plasma shielding takes place.

If we calculate the plasma frequency (f_p) for each energy using equation (5), we see that the frequency increases with laser pulse energy. Finally, use equation (4) to calculate the Debye number (N_D) for each laser pulse energy. Table 1 shows that all plasma parameters (λ_D, f_p and n_e) were measured and met plasma standards. This demonstrates that because f_p is proportional to ne and grows as ne drops while λ_D increases.

Table 1
Plasma parameters of Sn with different energy lasers.

E	Te (eV)	FWHM	ne*1018 (cm-3)	fp (Hz) *1012	λD *10-5(cm)	Nd
400	1.286	2.200	1.65	11.535	0.066	1.947
500	1.459	2.500	1.88	12.296	0.066	2.207
600	1.661	3.000	2.25	13.470	0.064	2.448
700	1.819	3.200	2.40	13.912	0.063	2.715

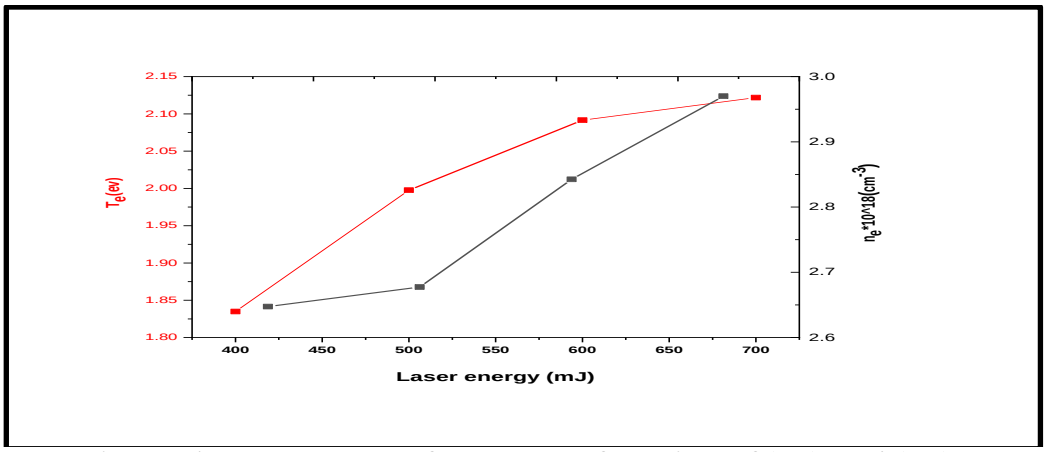

Figure 5. Laser energy for Sn as a function of (Te) and (ne).

Figure (7) indicates the electron temperature and electron density for tin and chromium calculated from Boltzmann diagram Equation 1. Since the laser top strength will increase the possibility of ionizing collisions with electron strength in all metals, it changed into located to boom with laser power. Also temperature and electron density. Electron temperature is exceedingly depending on top laser power, as it's far the supply of goal evaporation, atomization, and ionization all through focusing.

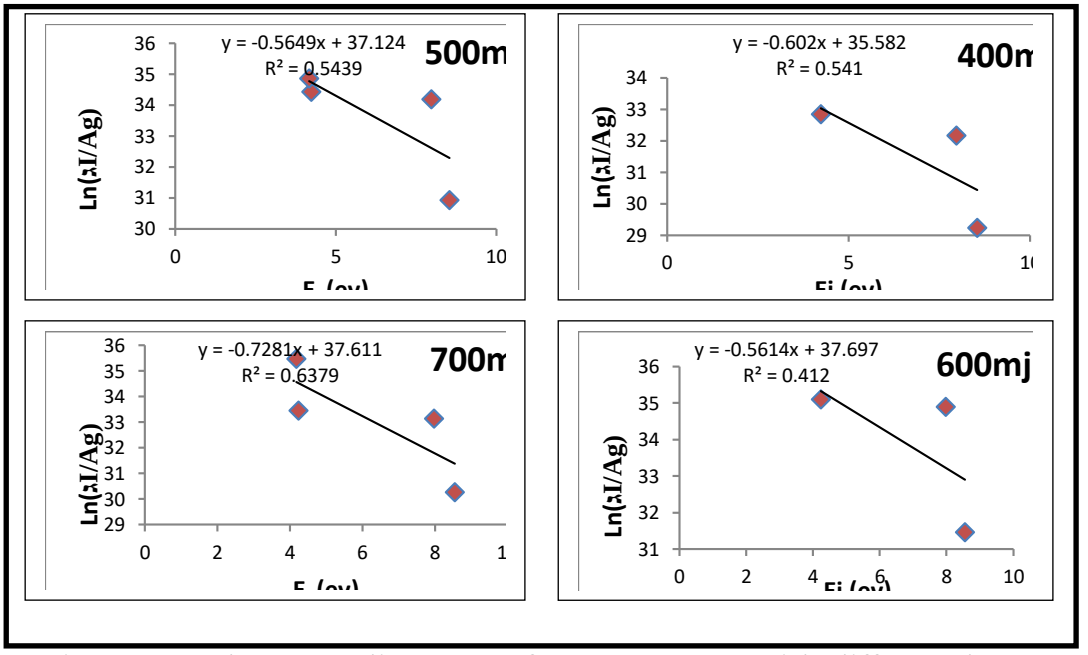

Figure 6. Boltzmann diagrams of Sn-Cr targets with different laser energies

It may be visible from Table 2 that the plasma frequency will increase with growing laser power, at the same time as the Debye period decreases.

Table 2.
Sn:Cr plasma parameters of lasers with different energies

E	Te (eV)	FWHM	ne*1018 (cm-3)	fp (Hz) *1012	λD *10-5(cm)	Nd
400	1.661	3.800	2.85	15.160	0.057	2.174
500	1.770	4.000	3.00	15.554	0.057	2.331
600	1.781	4.200	3.15	15.938	0.056	2.297
700	2.11505922	4.518	3.39	16.530	0.055	2.865

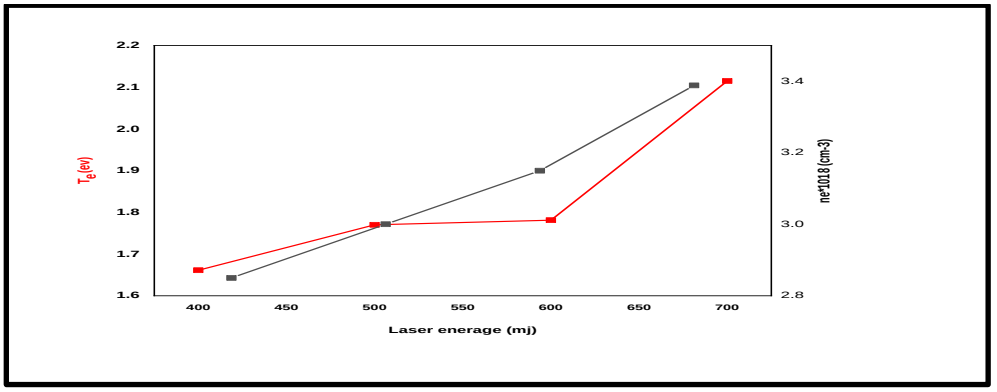

Figure 7. Variation of the laser energy of Sn:Cr with (Te) and (ne).

4. Conclusions

A laser with a wavelength of 1064nm and an energy range of (400–700) mJ is used to generate plasma Sn and Sn:Cr for research purposes. It seems that the spectral line intensities of the laser-caused plasma emission are pretty depending on the environment. Line intensities at distinct top powers extended with top laser power. Plasma parameters, electron temperature T_e, electron density (n_e) and plasma frequency (f_p) in Sn plasma and Sn:Cr plasma growth with laser power, at the same time as λ_D decreases.

References

Abbas, Ahmed K, and Saif I. Muslim. “Measurement the Parameters o Cadmium Oxide Plasma Induced by Laser.” International Journal of Recent Research and Applied Studies 4, no. 10 (2017): 66–72.

Ala F Ahmed, Mohammed R Abdulameer, Murad M Kadhim, Falah A-H. Mutlak, Plasma parameters of Au nano-particles ablated on porous silicon produced via Nd-YAG laser at 355 nm for sensing NH3 gas Optik Int. J. Light Electron Optics 2022 ,249, 168260–168269 .

E. Apaydin and M. Celik, “Investigation of the plasma parameters of a laboratory argon plasma source using a collisional radiative model with the comparison of

experimental and simulated spectra," Spectrochim. Acta Part B At. Spectrosc., vol. 160, p. 105673, 2019.

Hanif, M., and M. Salik. "Optical Emission Studies of Sulphur Plasma Using Laser Induced Breakdown Spectroscopy." Optics and Spectroscopy (English Translation of Optikai Spektroskopiya) 116, no. 2 (2014): 315–23. https://doi.org/10.1134/S0030400X1402009X.

Harilal, S. S., Beau O'Shay, Mark S. Tillack, and Manoj V. Mathew. "Spectroscopic Characterization of Laser-Induced Tin Plasma." Journal of Applied Physics 98, no. 1 (2005): 1–7. https://doi.org/10.1063/1.1977200.

Haverkamp, J., R. M. Mayo, M. A. Bourham, J. Narayan, C. Jin, and G. Duscher. "Plasma Plume Characteristics and Properties of Pulsed Laser Deposited Diamond-like Carbon Films." Journal of Applied Physics 93, no. 6 (2003): 3627–34. https://doi.org/10.1063/1.1555695.

Kramida, A, Ralchenko, Yu, Reader J and NIST ASD Team 2017 National Institute of Standards and Technology (NIST) Atomic spectra database 5.

Madyan A. Khalaf, Baida M. Ahmed , Kadhim A. Aadim, "Spectroscopic Analysis of CdO1-X: SnX Plasma Produced by Nd:YAG Laser"Iraqi Journal of Science, Vol. 61, No. 7, pp: 1665-1671 (2020).

Maryam M. Shehab, Kadhim A. Aadim,"Spectroscopic Diagnosis of the CdO:CoO Plasma Produced by Nd:YAG Laser", Iraqi Journal of Science, 2021, Vol. 62, No. 9, pp: 2948-2955,2021.

N. M. Shaikh, Y. Tao, R. A. Burdt, S. Yuspeh, N. Amin, and M. S. Tillack,"Spectroscopic studies of tin plasma using laser induced breakdown spectroscopy," in Journal of Physics: Conference Series, 2010, vol. 244, no. 4, p. 42005.

Wadaa S. Hussein, Ala F. Ahmed, K.A. Aadim, Influence of laser energy and annealing on structural and optical properties of CdS films prepared by laser induced plasma. Iraqi Journal of Science. 61(6), 1307–1312, 2020.